Desalination and Water Treatment
www.deswater.com

doi: 10.5004/dwt.2017.20932

80 (2017) 203–213
June

Removal of Ni(II), Cu(II), and Zn(II) ions from aqueous solution using *Tetraselmis* sp. biomass modified with silica-coated magnetite nanoparticles

Buhani*, Rinawati, Suharso, Dewa Putu Yuliasari, Suripto Dwi Yuwono

Department of Chemistry, Faculty of Mathematic and Natural Sciences, University of Lampung, Jl. Soemantri Brojonegoro No. 1, Bandar Lampung 35145, Indonesia, Tel. +62721704625; Fax: +62721702767; emails: buhani_s@yahoo.co.id (Buhani), rinawati@fmipa.unila.ac.id (Rinawati), suharso_s@yahoo.com (Suharso), dewa_yulianasari@yahoo.co.id (D.P. Yuliasari), suripto.dwi@fmipa.unila.ac.id (S.D. Yuwono)

Received 9 January 2017; Accepted 14 May 2017

ABSTRACT

Modification of algae–silica (AS) hybrid material from *Tetraselmis* sp. biomass (AS) was performed through a sol–gel simultaneous process and coated with Fe_3O_4 magnetite nanoparticles (MNPs). Algae–silica hybrid material from *Tetraselmis* sp. biomass-coated MNPs (AS-MNPs) were used as adsorbents of heavy metal ions. The adsorption processes of Ni(II), Cu(II), and Zn(II) ions with AS and algae-silica-magnetite nanoparticles (AS-MNPs) fit pseudo-second-order kinetic models. The rate constant and adsorption capacity of Ni(II), Cu(II), and Zn(II) ions for AS-MNPs obtained from these experiments were higher than those of AS. AS-MNPs material is an effective adsorbent and can be used to absorb heavy metal ions in solution.

Keywords: Tetraselmis sp.; Adsorption–desorption; Silica-coated magnetite; Heavy metals

1. Introduction

Heavy metal contamination from wastewater in the environment is a serious problem that needs to be controlled to save our planet. Several heavy metals found in industrial wastewater, such as Cd, Cu, Ni, Pb, Hg, Ag, Cr, and Zn, are not able to be degraded biologically or chemically in the environment [1–5].

The use of algae biomass as a heavy metal adsorbent material has been extensively developed because algae biomass contains several active groups that can serve as ligands to bind metal ions [6–8]. Several of the active groups in algae biomass consist of carboxyl, amino, hydroxyl, phosphate, and sulfate groups [9–14]. Algae biomass can adsorb metal ions by forming complexes between metal ions and functional groups, such as –COOH (the main component of polysaccharides) and peptide groups (–CO, $–NH_2$, and $–CONH_2$; the main components of pectins and proteins) acting as electron-pair donors for metal ions [15–17]. However, the ability of algae to adsorb metal ions is limited by several obstacles, such as their small size, low density, and easy degradation by other microorganisms [18,19].

Thus, algae biomass cannot be used directly in an adsorption column because it is soft and not granulated [20,21]. To control these problems, a method from a previous study is applied, immobilization of algae biomass using various supporting polymers.

Improvement of the physical and chemical qualities of algae biomass could be performed by immobilization using a supporting matrix, such as silica [22], through a cross-linking technique with epichlorohydrin or oxidization by potassium permanganate [23] and immobilization with sodium alginate [24]. Silica gel is a supporting matrix that is usually used for algae biomass immobilization. The use of silica as a supporting matrix has some reasons for use, such as it is easy to produce, easy to modify (geometry structure and surface chemical characteristic), stable, hydrophilic, and has a low cost of production. In addition, silica has a silanol group (Si–OH) that can interact in simple or complex formations [25,26].

* Corresponding author.

Immobilization of algae biomass using a silica matrix has been successfully used to increase the adsorption capacity of metal ions; immobilization of *Sargassum duplicatum* algae biomass [21] and *Nannochloropsis* sp. [22] with a silica supporting matrix has successfully increased the adsorption capacity and selectivity of binding metal ions. However, in application as an adsorbent material for continuous absorption, there is a problem with flocculants appearing and inhibiting the metal separating process from solution, producing environmentally unfriendly by-products [27–29]. Because of this issue, it is important to perform further modifications of algae biomass to increase its ability as a metal ion adsorbent.

Currently, synthesis of an adsorbent using the silica–magnetite coating technique has been developed because adsorbent quality increases can be carried out by coating MNPs on silica as a supporting matrix [30–34]. The silica coating technique with the use of a magnet is an environmentally friendly technique because it does not result in contaminated products. This technique also accelerates the metal separating process from solution because the adsorbent has magnetic characteristics [35,36]. By using this technique, good outcomes will be obtained because the adsorbent has a large capacity and selectivity for target metal ions and the ability to quickly separate the target metal [37–42]. The algae biomass contains organic groups, such as polysaccharides and proteins [15,17,43], that can be hybridized with silica-coated MNPs to produce an effective adsorbent to reduce metal ion concentrations for industrial or environmental applications.

In this paper, modification of the *Tetraselmis* sp. algae biomass with a hybrid process of algae biomass–silica coated MNPs that are formed by a sol–gel simultaneous process followed by coating with MNPs has been performed, and its application as a heavy metal adsorbent of Ni(II), Cu(II), and Zn(II) ions based on kinetic and isotherm adsorption aspects is evaluated. The adsorption kinetics was studied with pseudo-first-order and pseudo-second-order kinetic models. The ability of AS-MNPs to absorb heavy metals was evaluated using the Langmuir and Freundlich adsorption isotherm models. The endurance of the material upon reuse was investigated by repeatedly performing the adsorption–desorption process.

2. Experimental methods

2.1. Materials

Tetraselmis sp. biomass was taken from the Lampung Sea Cultivation Bureau (Balai Besar Budidaya Laut Lampung), Indonesia. Chemical reagents were purchased from Merck Co., Inc. (Germany), and consisted of tetraethyl orthosilicate (TEOS), ethanol, NH_3, HCl, $Ni(NO_3)_2 \bullet 4H_2O$, $Cu(NO_3)_2$, $Zn(NO_3)_2 \bullet 6H_2O$, $FeCl_3 \bullet 6H_2O$, $FeSO_4 \bullet 7H_2O$, Na_2EDTA, CH_3COOH, and CH_3COONa.

2.2. Synthesis of MNPs

Magnetite nanoparticle material was synthesized based on the method reported by Jiang et al. [44]. An amount of 5.56 g (0.020 mol) of $FeSO_4 \cdot 7H_2O$ and 6.48 g (0.024 mol) of $FeCl_3 \cdot 6H_2O$ were dissolved in 20 mL of distilled water and then added to a three-necked bottle under a nitrogen atmosphere. The solution was stirred until homogeneous, a 5% NH_3 solution was added to water dropwise until pH 8, and the solution was then left at room temperature for 2 h. The resultant product was neutralized with water and dialyzed for 48 h to produce MNPs.

2.3. Synthesis of algae–silica–Fe_3O_4 (AS-MNPs)

Five milliliters of TEOS was placed into 2.5 mL of water, to which 0.1 g of MNPs was added; they were then removed into a plastic bottle and stirred for 30 min. Then, drops of HCl were added until pH 2 (solution A). In the another bottle, 0.4 g of *Tetraselmis* sp. algae biomass was mixed with 5 mL of ethanol, and the mixtures were stirred for 30 min (solution B). Solution A was mixed with solution B by stirring to produce a gel. The gel obtained was left for 24 h, cleaned with water and ethanol until the filtrate pH was close to 7, and then dried in an oven at 40°C until its weight was constant. Dried material was ground and sieved through a sieve of 200 mesh. Synthesis of AS was performed by a similar procedure used to produce AS-MNPs, but without the addition of MNPs.

2.4. Analysis and characterization of the adsorbent

The synthesis resulted in a material that was characterized by an infrared spectrophotometer (IR) Prestige-21 Shimadzu to identify functional groups that existed in the material. The crystal structure of the material was analyzed by x-ray diffraction (XRD) (Shimadzu 6000); the surface morphology and constituent elements were investigated by scanning electron microscopy and energy-dispersive X-ray analysis (SEM–EDX) (JSM 6360 LA). The metal ion concentrations were calculated using atomic absorption spectrophotometer (AAS) (Perkins Elmer 3110).

2.5. Adsorption experiments

Adsorption processes were performed to investigate interactions according to the pH, contact time, and adsorption isotherm. The influence of pH on adsorption was studied by interacting each adsorbent (50 mg) in a series of glass reaction tubes with 25 mL of each solution of Ni(II), Cu(II), and Zn(II) at a concentration of 100 mg L^{-1} for 60 min over a pH range of 2–8 with giving buffer solutions each of 0.1 M CH_3COONa/HCl (for low pH) and CH_3COONa/CH_3COOH (for high pH).

The effect of the contact time was tested at the optimum pH in a similar manner as that of the pH adsorption influence tests, with interaction time intervals between 0 and 90 min.

The adsorption isotherms of Ni(II), Cu(II), and Zn(II) ions were studied by interacting 50 mg of adsorbent removed in a series of glass reaction tubes with the addition of 25 mL each of a Ni(II), Cu(II), and Zn(II) ion solution at various concentrations between 0.0 and 400.0 mg L^{-1}. Adsorption was carried out in a batch system using a magnetic stirrer at the optimum pH and time at a temperature of 27°C. Then, the solution was centrifuged and the filtrate was removed to assess the metal concentration that remained in solution by AAS analysis.

The amount of metal adsorbed per mass unit of adsorbent was calculated using Eq. (1):

$$q = \frac{(C_o - C_t)}{m} \times V \quad (1)$$

where C_o and C_t (mg L^{-1}) are the metal ion concentration before and after the adsorption process, respectively; m is the amount of adsorbent (g); and V is the solution volume (L).

To evaluate the adsorption parameter model obtained, analysis of non-linear regression was performed, investigating the correlation between the amount of metal ion adsorbed experimentally and estimated from a kinetic and adsorption isotherm model. These evaluations were applied by determining the root mean squared error (RMSE; Eq. (2)) and the use of the Chi-square test (χ^2; Eq. (3)) [45,46]:

$$\text{RMSE} = \sqrt{\left(\frac{1}{m-2}\right)\sum_{i=1}^{m}\left(q_{i,\text{exp}} - q_{i,\text{cal}}\right)^2} \quad (2)$$

$$\chi^2 = \sum_{i=1}^{m}\frac{\left(q_{i,\text{exp}} - q_{i,\text{cal}}\right)^2}{q_{i,\text{exp}}} \quad (3)$$

where $q_{i,\text{exp}}$ and $q_{i,\text{cal}}$ are each obtained from experiments and estimated via kinetic and adsorption isotherm equations, respectively, and m is the number of observations in the experimental isotherm. A smaller RMSE value indicates a better curve fit; moreover, if the data obtained from the models are close to the experimental results, χ^2 will be a small number [45,47].

2.6. Regeneration and reusability

A single cycle consists of adsorption followed by desorption (Cu(II) ion concentration of 400 mg L^{-1}, AS-MNPs mass of 50 mg, interaction time of 60 min, pH of 6, and temperature of 27°C). The Cu(II) ions adsorbed on the AS-MNPs were released using 0.1 M Na_2EDTA. Then, the AS-MNPs were cleaned by water to reach a neutral pH and dried in an oven at a temperature of 40°C. The experiment was repeated for five cycles to regenerate the spent adsorbent. The percentage (%) of metal ions adsorbed and desorbed was determined using Eqs. (4) and (5).

$$\text{Adsorption \%} = \frac{C_o - C_t}{C_o} \times 100 \quad (4)$$

$$\text{Desorption \%} = \frac{\text{Amount of metal desorbed by the reagent (mg g}^{-1})}{\text{Amount of metal adsorbed onto the adsorbent (mg g}^{-1})} \times 100 \quad (5)$$

3. Results and discussion

3.1. Synthesis and characterization

Synthesis of AS-MNPs was performed by a simultaneous sol–gel process with an MNP coating technique, as described in Fig. 1. The reaction started with TEOS hydrolysis under acidic conditions to produce $Si(OH)_4$ and continued with the formation of silicate anions resulting from the dissociation of H^+ from –SiOH groups. Before the sol–gel process occurred, hybridization occurred between silica and the *Tetraselmis* sp. biomass, accompanied by an MNP coating, which was followed a condensation reaction to produce AS-MNPs in the form of gel.

Surface modification of the algae–silica hybrid from the *Tetraselmis* sp. biomass-coated with MNPs was performed based on the identification of functional groups by IR spectrophotometry, material diffraction model using XRD, surface morphology and constituent elements using SEM–EDX.

The IR spectra of the MNPs, silica–MNPs, *Tetraselmis* sp. algae biomass, AS, and AS-MNPs are displayed in

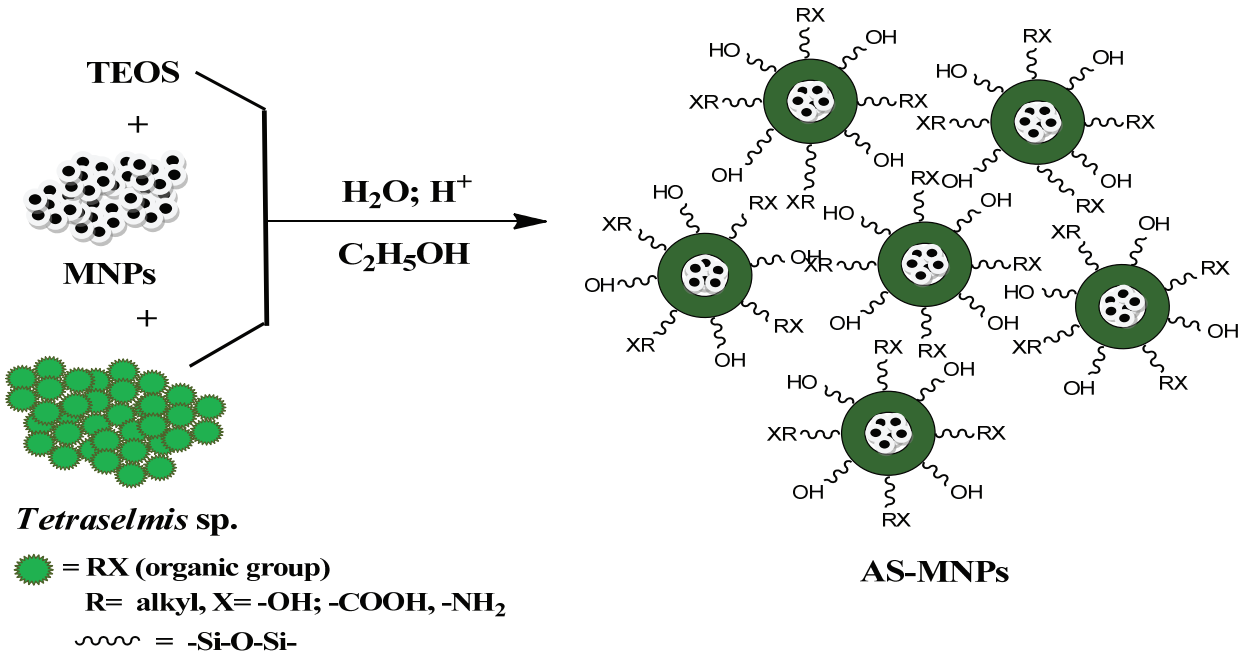

Fig. 1. Synthesis of AS-MNPs from the hybridization of silica–algae biomass coated with MNPs.

Fig. 2. From this figure, that overlapping O–H and N–H group stretching vibrations produce the same IR absorption band at 3,425.58 cm^{-1} [43,48]. These bands indicate the existence of –OH group from polysaccharides or –NH group from proteins contained in the *Tetraselmis* sp. biomass. It was also reported that the bending bands at 1,635.16 and 1,442.75 in the cellulose spectrum are characteristic of cellulose from an algae biomass [43,49]. The band at 1,072.42 demonstrates the presence of –C–O groups of a cellulosic structure, indicating characteristic bands from the *Tetraselmis* sp. biomass that play a role as active groups to bind metal ions.

Furthermore, the identification of material functional groups by IR spectrophotometry (Fig. 2) shows that hybridization has occurred between the silica matrix and algae biomass for AS, as well as for AS-MNPs. These facts were indicated by the absorption bands of the AS and AS-MNPs that occurred at approximately 2,931.30 cm^{-1}, characterizing a stretching vibration of $–CH_2$ groups derived from the *Tetraselmis* sp. algae biomass (Fig. 2(c)) [22]; at 462.92 cm^{-1}, showing bending vibrations of siloxane groups (Si–O–Si); and near 786.96 cm^{-1}, indicating a symmetric stretching vibration of Si–O from siloxane. A strong absorption band at 1,072.2 cm^{-1} shows the asymmetric stretching vibration of Si–O from siloxane (Si–O–Si) [50]. These facts were strengthened by the disappearance of the stretching vibration of Si–O from Si–OH at 964.41 cm^{-1} caused by the decrease of silanol groups because of condensation occurring with the *Tetraselmis* sp. algae biomass (Fig. 2(b)). In this research, the presence of MNPs in the IR spectra of AS-MNPs cannot be clearly observed. The occurrence of MNP-coating on AS-MNPs can be identified by observing the XRD diffraction model and element constituents contained in the spectrum of EDX.

Fig. 3 displays the difference in the XRD patterns between MNPs, AS, and AS-MNPs. The XRD pattern of MNPs (Fig. 3(a)) fit to the data base of Joint Committee on Powder Diffraction Standards (JCPDS), the XRD pattern of a standard magnetite crystal with spinel structure has five characteristic peaks at 2θ = 30.5°, 35.9°, 43.6°, 57.5°, and 62.8° [32,44]. In AS (Fig. 3(c)), there is no XRD pattern; however, this pattern occurs in MNPs (Fig. 3(a)), which shows that this material is a non-crystal structure [40] or AS is amorphous because it is dominated by SiO_2, which is characterized as amorphous [29]. In AS-MNPs, there (Fig. 3(d)) are XRD patterns with large intensities at 2θ = 30.5° and 35.9°, which are characteristic of MNPs [28,39]; this shows that MNPs occur in AS-MNPs.

The results of the surface morphology according to SEM (Fig. 4) analysis show that there is a difference in the surface morphology between AS (Fig. 4(b)) and AS-MNPs (Fig. 4(c)).

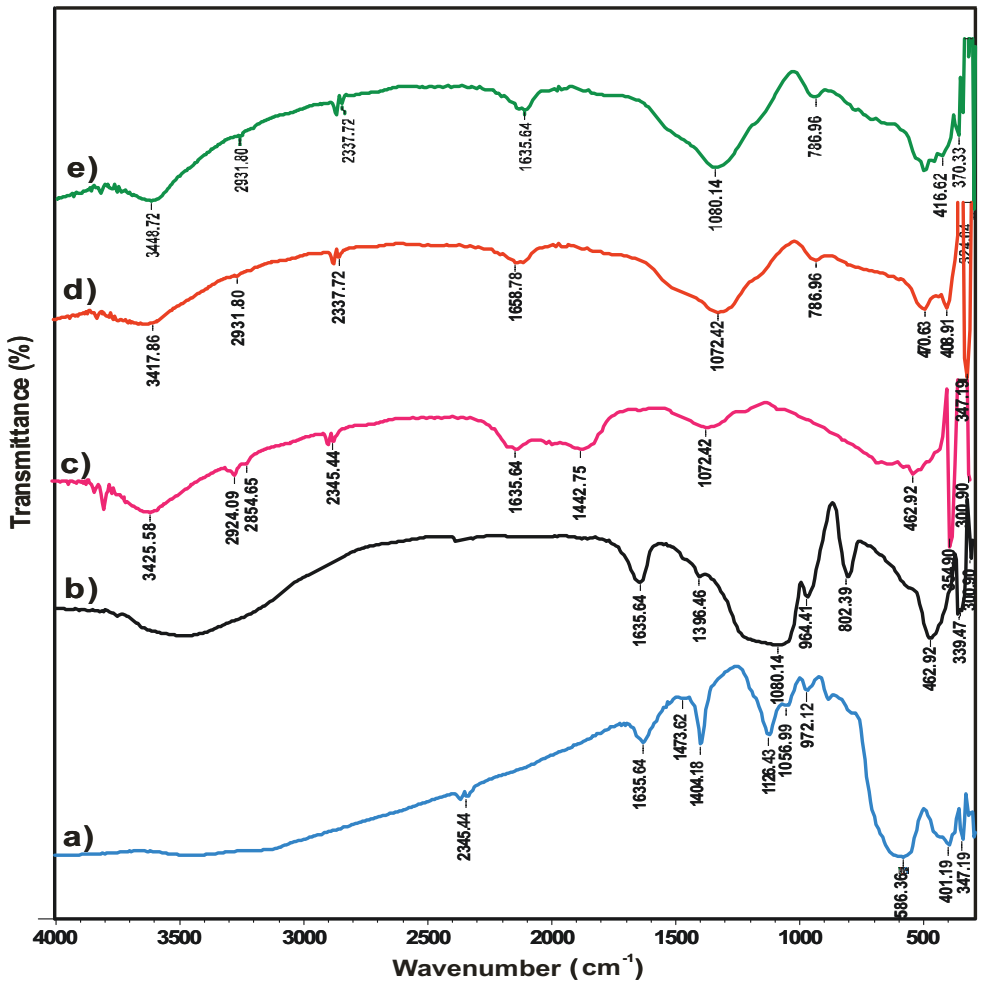

Fig. 2. IR spectra of (a) MNPs, (b) silica–MNPs, (c) *Tetraselmis* sp. algae biomass, (d) AS, and (e) AS-MNPs.

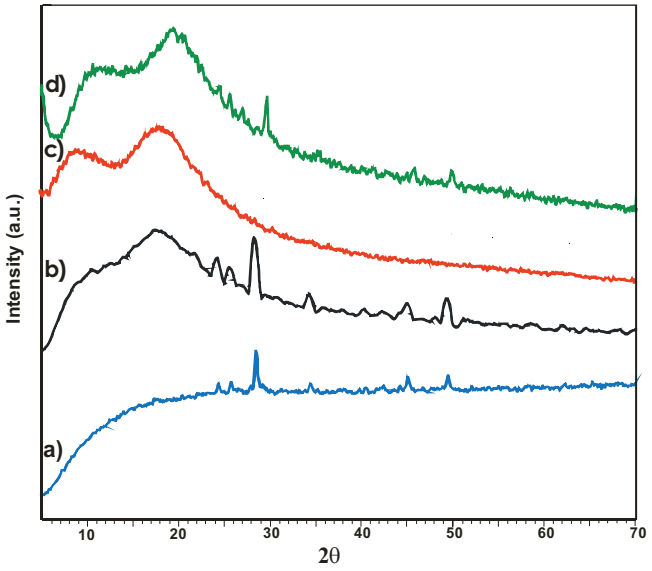

Fig. 3. Typical XRD patterns of (a) MNPs, (b) silica–MNPs, (c) AS, and (d) AS-MNPs.

The surface morphology of AS-MNPs is observed to have more contrast than that of MNPs (Fig. 4(a)) because of the existence of MNPs in the materials. The existence of MNPs containing high atomic numbers in these materials causes a higher acceleration of atoms, resulting in a higher intensity contrast caused by broad scattering. In Fig. 4, the structure of AS-MNPs gives smaller aggregate than the structure of MNPs because on the AS-MNPs existed contribution of amorphous silica and organic compounds from *Tetraselmis* sp. algae biomass. Change of the material structure was also supported by analisys of IR spectra discussed previously stating that on MNPs existed silica as matrix and also functional groups from *Tetraselmis* sp. biomass. From the XRD analysis, it can be observed that the changes in the structure of amorphous AS tends to be crystalline on AS-MNPs caused the existency of MNPs which is crystalline. Element composition of each material can be detected from EDX spectra of MNPs, AS, and AS-MNPs are listed in Figs. 4(d)–(f). Constituents such as C, Si, and O are present in the EDX spectra of AS and AS-MNPs (Figs. 4(e) and (f)). The magnetite coating was confirmed by the presence of Fe in the EDX spectra of the AS-MNPs.

3.2. Influence of the interaction pH

The effect of the solution pH was studied by interacting each solution of Ni(II), Cu(II), and Zn(II) ions on AS-MNPs at different pHs from 2 to 8 (Fig. 5). In general, the adsorption of these metal ions is optimal at pH 6. At a lower pH (<6), the adsorption process was not yet optimal because the active groups on AS-MNPs can lead to protonation, causing hydrogen ions (H^+) and hydronium ion (H_3O^+) to bind, decreasing the presence of active groups on the adsorbent, which are needed to complex with metals in solution [13,37].

At a pH of approximately 6, the adsorption process tends to be optimal because the active sites on AS-MNP exist in a neutral formation as amino, hydroxyl, and carboxyl groups derived from the algae biomass [11,12,14]. This formation can play a role as an electron-pair donor and result in strong interactions with Ni(II), Cu(II), and Zn(II) metal ions. In addition, the possibility still exists for –OH and –Si–O–Si– groups to occur on AS-MNPs, which also play a role as donors in this condition because they tend to be negatively charged.

At pH > 6, the adsorption process starts to decrease because Ni(II), Cu(II), and Zn(II) metal ions tend to hydrolyze to form metal hydroxyl species precipitates [16,32]. Moreover, under these conditions, the material surface becomes negatively charged, resulting in repulsion forces between the material surface and metal ions. Ultimately, the adsorption process decreases.

Optimum condition of adsorption process of Ni(II), Cu(II), and Zn(II) ions on MNPs that happened at pH 6 tends to be in line with the value of pH of zero point charge (pH_{ZPC}) determined by previous research [37,61] on the adsorbents based silica–magnetite nanoparticle and Fe_3O_4/cyclodextrin polymer nanocomposites with the value of pH_{ZPC} 6.2 and 4.4, respectively. If medium pH above pH_{ZPC} ($pH > pH_{PZC}$), the adsorbent surface will be negative charge caused by deprotonation of functional groups or adsorption of hydroxyl species. If medium pH is lower than pH_{ZPC} ($pH < pH_{PZC}$), the adsorbent surface will be positive charge resulted from protonation of functional groups.

3.3. Adsorption kinetics

In Fig. 6, it can be observed that, generally, the adsorption of Ni(II), Cu(II), and Zn(II) ions on AS and AS-MNPs runs relatively fast. For the first 15 min, the adsorption rises very sharply, but after a subsequent15 min, adsorption slows and finally reaches a constant at 60 min. Possibly, at this stage, the adsorption process has reached equilibrium and the addition of more time does not lead to significant increases in metal ion adsorption.

To investigate the kinetic model for the adsorption process of Ni(II), Cu(II), and Zn(II) metal ions on AS and AS-MNPs, the data obtained in Fig. 6 were evaluated with pseudo-first-order and pseudo-second-order kinetic models [13,51]. Linear equations of the used pseudo-first-order (Eq. (6)) and pseudo-second-order (Eq. (7)) kinetic models are described below:

$$\log(q_e - q_t) = \log q_t \frac{k_1}{2.303} t \tag{6}$$

$$\frac{t}{q_t} = \frac{1}{k_2 q_e^2} + \frac{t}{q_e} \tag{7}$$

where q_t and q_e (mg g^{-1}) are total metal ions adsorption capacity at time, t, at equilibrium and k_1 and k_2 are the first-order and second-order rate constants, respectively. The kinetics experimental data and their parameters are displayed in Table 1.

From the data in Table 1, it can be stated that the kinetic models of Ni(II), Cu(II), and Zn(II) ions on AS and AS-MNPs tend to follow a second-order kinetic model, as shown by the correlation coefficient value (R^2) close to 1 and small RMSE and χ^2 values. These kinetic parameters indicate that the adsorption process runs fast and is greatly affected by

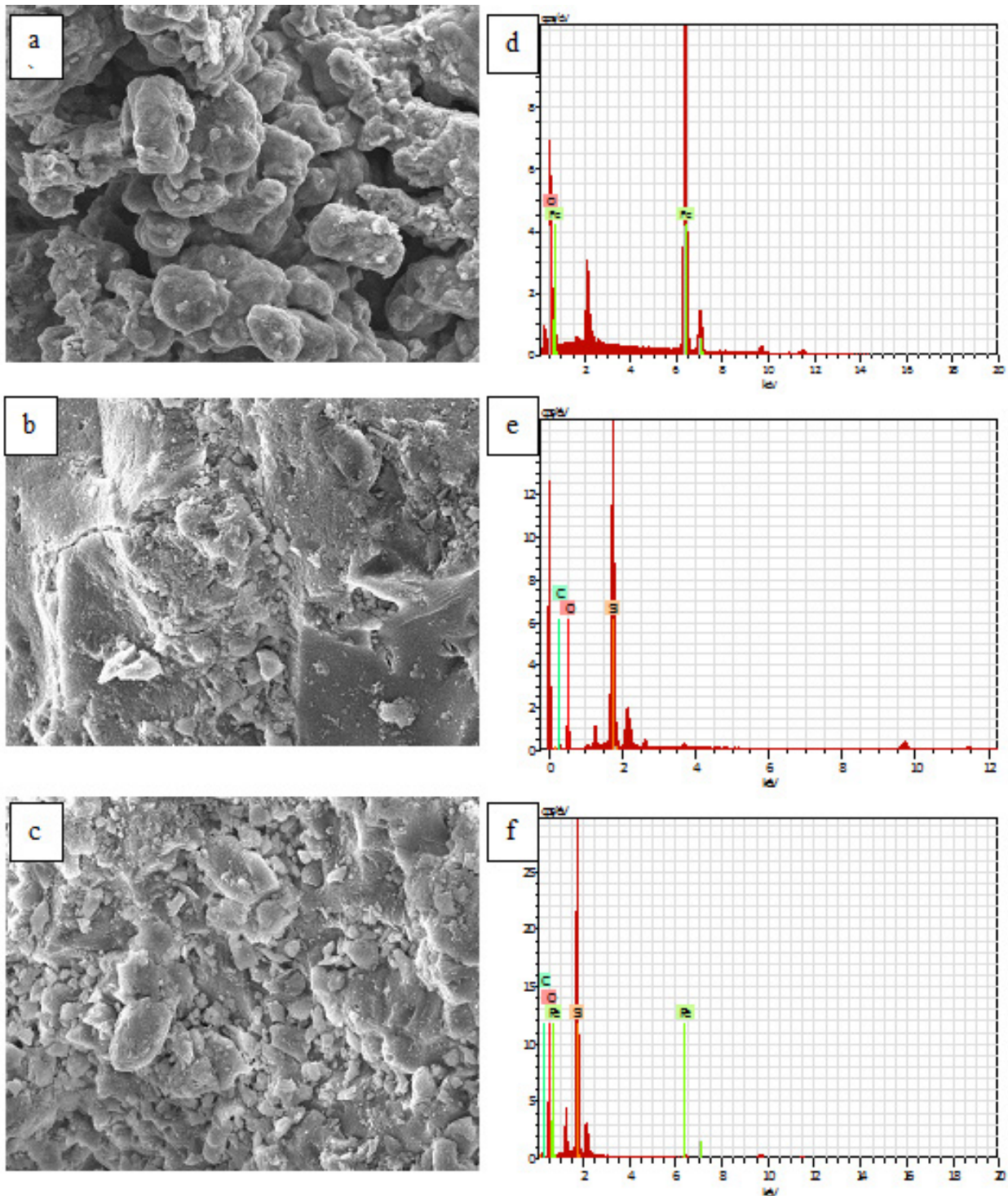

Fig. 4. SEM images and EDX spectra of (a) and (d) MNPs; (b) and (e) AS; and (c) and (f) AS-MNPs.

metal ions and adsorbents. Based on the pseudo-second-order rate constant value (k_2) for each ion (Table 1), it can be observed that the k_2 values on AS-MNPs are higher than on AS, namely, 0.470 Ni(II), 0.522 Cu(II), and 0.478 Zn(II) g mmol^{-1} min^{-1}.

The increasing rate of adsorption on AS-MNPs is caused by the existence of MNPs resulting from a magnetic adsorbent; therefore, the interaction between metal ions and adsorbents runs fast, as reported in the pseudo-second-order adsorption kinetics of several metal ions by adsorbents, including amine-functionalized mesoporous Fe_3O_4 nanoparticles [30] and amine-functionalized silica magnetic [32], nanomagnetic cellulose hybrid [39], and spherical Fe_3O_4/bacterial cellulose nanocomposites [52].

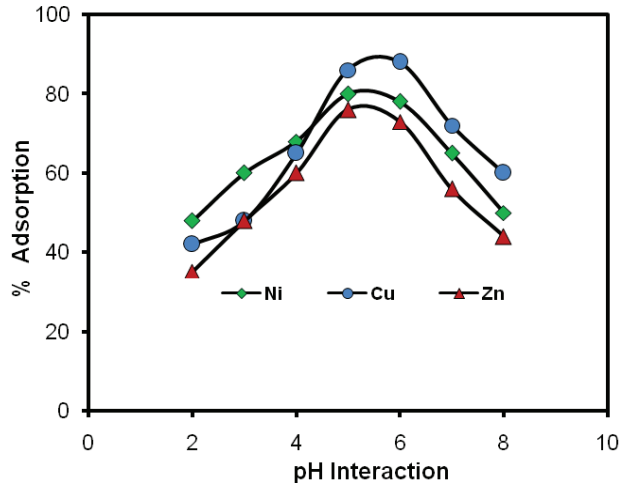

Fig. 5. Percentage of Ni(II), Cu(II), and Zn(II) ions adsorbed by AS-MNPs at a pH interval of 2–8.

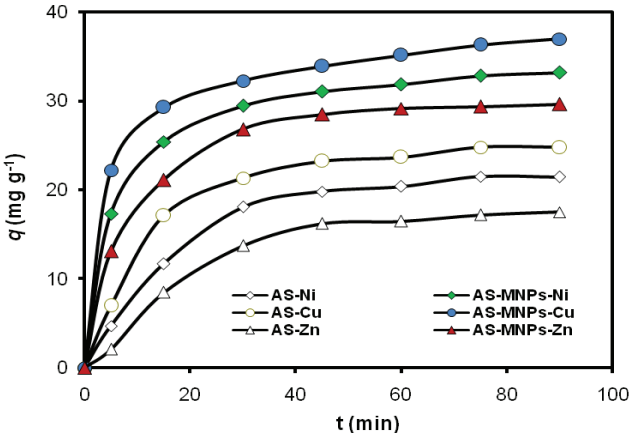

Fig. 6. Effect of the interaction time vs. the amount of Ni(II), Cu(II), and Zn(II) metal ions adsorbed on AS and AS-MNPs at pH 6 (concentration of 100 mg L^{-1} and temperature of 27°C).

3.4. Adsorption isotherm

The isotherm models and adsorption parameters of Ni(II), Cu(II), and Zn(II) ions on AS and AS-MNPs were determined by analyzing the adsorption data using the adsorption model of Langmuir (Eq. (8)) and a Freundlich isotherm (Eq. (9)):

$$\frac{1}{q_e} = \frac{1}{q_m K_L C_e} + \frac{1}{q_m} \tag{8}$$

$$\log q_e = \log K_f + \frac{1}{n}\log C_e \tag{9}$$

where q_e is the amount of adsorbate on the adsorbent at equilibrium (mg g^{-1}), C_e (mg L^{-1}) is the equilibrium concentration of the adsorbate, q_m (mg g^{-1}) is the maximum adsorption capacity, and K_L (L mg^{-1}) is the Langmuir adsorption equilibrium constant. The values of K_L and q_m were calculated from the slope and intercept of a plot of $1/q_e$ vs. $1/C_e$, respectively. In the Freundlich isotherm model, K_f indicates the adsorption capacity and n indicates the heterogeneity factor for which a favorable adsorption is larger than one ($n > 1$). The values of K_f and n can be obtained from plotting $\log q_e$ vs. $\log C_e$.

The adsorption parameters of Ni(II), Cu(II), and Zn(II) ions on AS and AS-MNPs are listed in Table 2. Generally, from the adsorption isotherm models, it can be observed that the amount of metal ion adsorbed on AS-MNPs is higher than that on AS. In addition, in Fig. 7, it can be observed that the plot of the relationship between the amount of metal adsorbed and the metal ion initial concentration estimated with the Langmuir (q Langmuir) equation are relatively fit to the experiment results (q_{exp}) compared with those from the Freundlich isotherm model (q Freundlich). This is also supported by the regression coefficient data (R^2) of each adsorption isotherm model for Ni(II), Zn(II), and Cu(II) on AS and AS-MNPs, as listed in Table 2, showing that the adsorption process of these metal ions tends to follow the

Table 1
Adsorption kinetic parameters of Ni(II), Cu(II), and Zn(II) ions on AS and AS-MNPs at a concentration of 100 mg L^{-1}, pH of 6, and temperature of 27°C

Adsorbents		AS			AS-MNPs		
Metal ions		Ni(II)	Cu(II)	Zn(II)	Ni(II)	Cu(II)	Zn(II)
Experiment value	$q_{e,exp}$ (mg g^{-1})	21.422	24.719	17.525	31.810	36.920	29.622
Pseudo-first-order	k_1 (min^{-1})	0.105	0.048	0.044	0.064	0.053	0.055
	$q_{e,cal}$ (mg g^{-1})	20.365	23.194	23.344	23.476	26.689	21.383
	R^2	0.959	0.911	0.962	0.953	0.827	0.899
	RMSE	0.079	0.089	0.059	0.062	0.083	0.077
	χ^2	0.075	0.057	0.039	0.031	0.045	0.040
Pseudo-second-order	k_2 (g $mmol^{-1}$ min^{-1})	0.209	0.318	0.397	0.480	0.522	0.478
	$q_{e,cal}$ (mg g^{-1})	19.544	23.004	15.890	30.519	35.586	28.248
	R^2	0.968	0.986	0.976	0.997	0.997	0.995
	RMSE	0.057	0.048	0.036	0.043	0.052	0.037
	χ^2	0.051	0.035	0.018	0.012	0.010	0.014

Table 2
Adsorption isotherm parameters of Ni(II), Cu(II), and Zn(II) ions on AS and AS-MNPs at an interaction time of 60 min, pH of 6, and temperature of 27°C

Adsorbents		AS			AS-MNPs		
Metal ions		Ni(II)	Cu(II)	Zn(II)	Ni(II)	Cu(II)	Zn(II)
Models	Parameters						
	q_{exp} (mg g^{-1})	40.400	48.39	39.200	76.800	85.400	74.600
	q_m (mg g^{-1})	41.921	52.955	40.869	83.843	90.780	81.738
Langmuir	$K_L \times 10^4$ (L mg^{-1})	2.395	3.648	3.476	2.445	4.732	3.138
	R^2	0.996	0.998	0.998	0.995	0.995	0.994
	RMSE	2.500	5.567	2.068	2.572	2.633	0.707
	χ^2	0.168	0.865	0.644	0.840	0.783	0.497
Freundlich	K_f (mg g^{-1})	2.634	3.105	2.582	3.642	6.564	3.784
	n	1.761	1.786	1.845	1.503	1.767	1.534
	R^2	0.832	0.802	0.830	0.815	0.705	0.809
	RMSE	10.100	14.790	10.430	25.884	14.790	23.711
	χ^2	22.331	37.367	23.090	70.285	37.367	60.509

Langmuir adsorption isotherm model. In the Langmuir adsorption isotherm model, the R^2 values are closer to 1 and the RMSE and χ^2 values are smaller than in the Freundlich model.

The Langmuir adsorption isotherm model assumes that on the adsorbent surface, there are a definite number of active sites that are comparable with the surface area, the surface of the adsorbent is uniform, and the adsorption process occurs in a monolayer [53–55]. Therefore, it can be stated that the adsorption process is dominated by the chemical interactions between metal ions and the adsorbent active sites. Interactions between metal ions and active sites on the algae–silica matrix biomass derived from *Tetraselmis* sp. completed with magnetic MNPs will raise the adsorbent rate and capacity for metal ions.

The adsorption process of metal ion AS-MNPs occurs according to complex formation among metal ions and functional groups, which play a role as electron-pair donors, as discussed in the adsorbent characterization results previously. In addition, the presence of MNPs on AS-MNPs causes a larger surface area on the adsorbent and easier separation of metal ions from media solution because of the existence of an external magnetic field from MNPs [41,56,57]. Moreover, the adsorption rate data (k_2) in Table 1 and Langmuir adsorption capacity values (q_m) in Table 2 show that there is an increasing order of metal ion adsorbed of Zn(II) < Ni(II) < Cu(II) ions on AS and AS-MNPs. These facts are also supported by the free energy involved in the adsorption processes as determined by Eq. (10) as follows:

$$\Delta G_{ads} = -RT \ln K_L \quad (10)$$

where ΔG_{ads} is change in Gibbs free energy (kJ mol^{-1}), R is the universal gas constant (8.314 J K^{-1} mol^{-1}), and T is the temperature (K). From the calculation of the results using Eq. (10), the ΔG_{ads} value at a temperature of 300 K for Ni(II), Cu(II), and Zn(II) ions on MNPs were obtained, respectively, at –32.275, –33.723, and –32.628 kJ mol^{-1}. The ΔG_{ads} data from this experiment are comparable with the adsorption energy (ΔG_{ads}) obtained from the adsorption of Cr(IV) ions by mesoporous silica–MNPs modified by 3-aminopropyltriethoxysilane of –34.60 kJ mol^{-1} at 298 K [41]. The negative values of ΔG_{ads} for the adsorption of Ni(II), Cu(II), and Zn(II) ions show that the adsorption is an exothermic process that runs spontaneously [41,42]. In aqueous media, metal ions will exist in the form of $[M(H_2O)_n]^{2+}$ so that the solvation energy ($-\Delta G_{solv}$) plays more of a role in metal ion mobility. A Cu(II) ion in aqueous media has a larger $-\Delta G_{solv}$ than that of Ni(II) and Zn(II) ions [58]. Therefore, Cu(II) ions have higher mobility in aqueous media, resulting in them being easier to be adsorbed by an adsorbent.

The adsorption capacity of Cu(II), Ni(II), and Zn(II) ions on AS-MNPs, as determined by the Langmuir model, is 83.843, 90.780, and 81.738 mg g^{-1}, respectively; if the adsorption capacity is compared with that of several adsorbents reported from the literature (Table 3), the adsorption capacity is not too different from that other adsorbents based on MNPs; however, AS-MNPs are environmentally friendly because they are derived from an algae biomass as a natural product that can be degraded and not produce dangerous by-products for the environment.

3.5. Regeneration and reusability

Material reusability to adsorb metal ions several times without inducing material structure damage and decreasing the adsorption capacity is an important parameter in determining the quality of a synthesized material; the more often it can be reused, the higher the quality of the material. To test the AS-MNPs material generated in this work, the adsorption–desorption process with Cu(II) ions was performed several times, as observed in Fig. 8. The adsorption–desorption results for Cu(II) ions with a 0.1 M EDTA eluent solution for four cycles did not significantly decrease the adsorption capacity. A decrease of the adsorption capacity occurred at

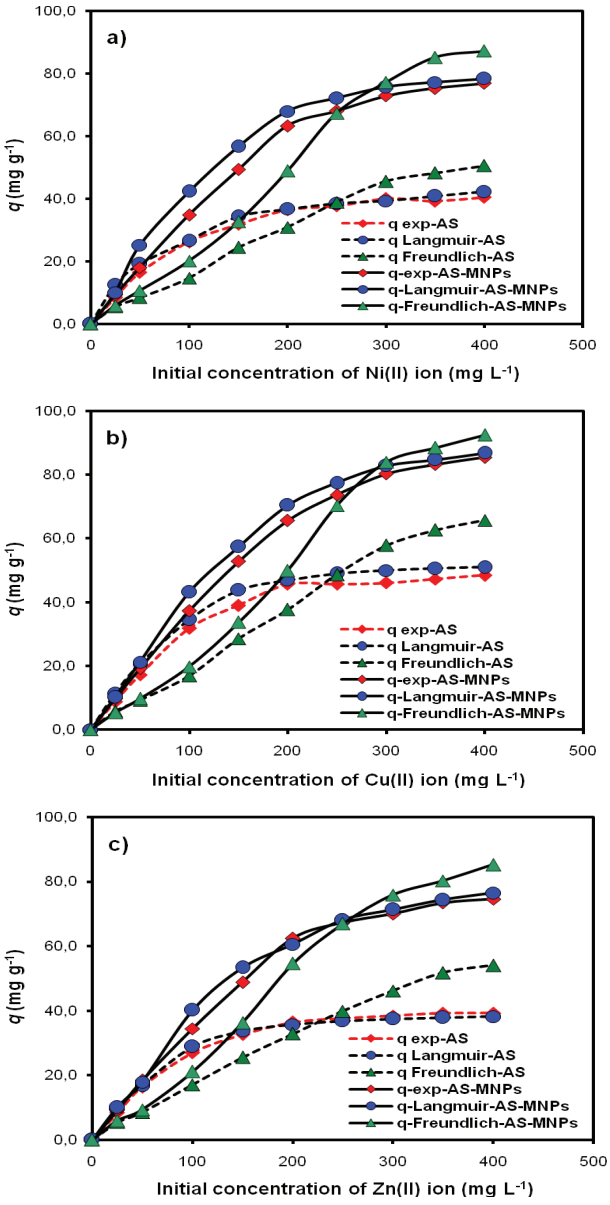

Fig. 7. Isotherm adsorption pattern of (a) Ni(II), (b) Cu(II), and (c) Zn(II) ions on AS and AS-MNPs based on experimental (q_{exp}) and estimation (q) results using adsorption isotherm equations.

the fifth reuse with a percentage of Cu(II) ions adsorbed on AS-MPNs of approximately 70.4% (Fig. 8). The decreasing of adsorption capacity is caused by the loss of active sites on MNPs and may be attributed to the detachment of the silica coating from the MNPs surface during the recycling process [32], as evidenced by the presence of dissolved silicate in the adsorption reaction solution of approximately 8.5%. The reusability data of AS-MNPs adsorbent may be used as a reference that the adsorbent can be reused and is efficient in adsorbing heavy metal ions in solution.

4. Conclusion

The modification of *Tetraselmis* sp. algae biomass hybridized with silica and magnetic nanoparticles has been performed successfully, and this biomass can be applied as an adsorbent of heavy metal ions, such as Ni(II), Cu(II), and Zn(II). The structure of AS-MNPs gives smaller aggregate than the structure of MNPs because on the AS-MNPs existed contribution of amorphous silica and organic compounds from *Tetraselmis* sp. algae biomass. Application of a simultaneous sol–gel and coating process with MNPs produced a magnetic and more homogeneous AS-MNPs material to increase the rate and adsorption capacity for

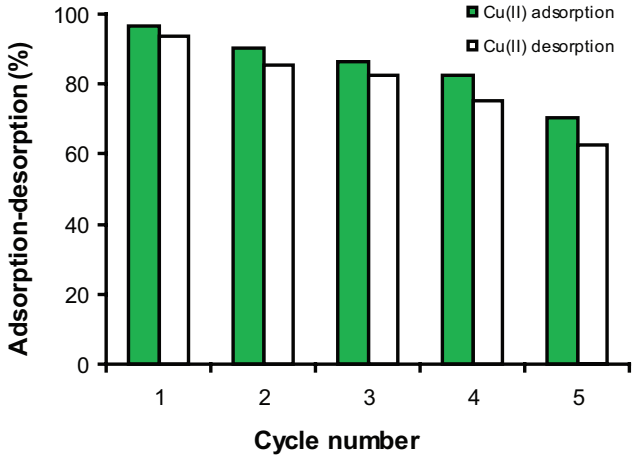

Fig. 8. Reusability number efficiency of the adsorption–desorption process of Cu(II) ions on AS-MNPs.

Table 3
Adsorption capacity of Ni(II), Cu(II), and ZN(II) ions on various adsorbents based on their magnetic properties

Adsorbents	Adsorption capacity of metal ions (mg g^{-1})			Reference
	Ni(II)	Cu(II)	Zn(II)	
$NH_2/SiO_2/Fe_3O_4$		10.41		[32]
Fe_3O_4/cyclodextrin polymer nanocomposites	13.20			[37]
Magnetic Cu(II) imprinted composite		71.36		[40]
Carboxymethyl-β-cyclodextrin-magnetic		47.20		[59]
Dimethylglyoxime/alumina-coated magnetite nanoparticles	9.72			[60]
Mesoporous silica-coated magnetic nanoparticles modified with 4-amino-3-hydrazino-5-mercapto-1,2,4-triazole		5.02		[61]
AS-MNPs	83.84	90.78	81.74	This work

metal ions. It can be concluded that AS-MNPs is an effective adsorbent and can be used to absorb heavy metal ions in solution.

Acknowledgments

This work was funded by the Directorate of Research and Community Services, Directorate General of Higher Education (DIKTI), Ministry of Research, Technology and Higher Education of the Republic of Indonesia from the Competency Research Grant/Hibah Kompetensi, with contract number: 79/UN26/8/LPPM/II/2016.

References

[1] L. Tran, P. Wu, Y. Zhu, S. Liua, N. Zhu, Comparative study of Hg(II) adsorption by thiol and hydroxyl containing bifunctional montmorillonite and vermiculite, Appl. Surf. Sci., 356 (2015) 91–101.
[2] Buhani, Narsito, Nuryono, E.S. Kunarti, Suharso, Adsorption competition of Cu(II) ion in ionic pair and multi-metal solution by ionic imprinted amino-silica hybrid adsorbent, Desal. Wat. Treat., 55 (2015) 1240–1252.
[3] Q. Xiao, Y. Sun, J. Zhang, Q. Li, Size-dependent of chromium (VI) adsorption on nano α-Fe_2O_3 surface, Appl. Surf. Sci., 356 (2015) 18–23.
[4] Suharso, Buhani, Biosorption of Pb(II), Cu(II) and Cd(II) from aqueous solution using cassava peel waste biomass, Asian J. Chem., 23 (2011) 1112–1116.
[5] M. Mukhopadhyay, S.B. Noronha, G.K. Suraishkumar, Kinetic modeling for the biosorption of copper by pretreated *Aspergillus niger* biomass, Bioresour. Technol., 98 (2007) 1781–1787.
[6] Buhani, Suharso, A.Y. Fitriyani, Comparative study of adsorption ability of Ni(II) and Zn(II) ionic imprinted amino-silica hybrid toward target metal in solution, Asian J. Chem., 25 (2013) 2875–2880.
[7] A.A. Al-Homaidan, H.J. Al-Houri, A.A. Al-Hazzani, G. Elgaaly, N.M.S. Moubayed, Biosorption of copper ions from aqueous solutions by *Spirulina platensis* biomass, Arabian J. Chem., 7 (2014) 57–62.
[8] Y.G. Bermüdez, I.L.R. Rico, O.G. Bermüdez, E. Guibal, Nickel biosorption using *Gracilaria caudata* and *Sargassum muticum*, Chem. Eng. J., 166 (2011) 122–131.
[9] K. Masakorala, A. Turner, M.T. Brown, Influence of synthetic surfactants on the uptake of Pd, Cd, and Pb by marine macroalga, *Ulva lactuca*, Environ. Pollut., 156 (2008) 897–904.
[10] K. Vijayaraghavan, M. Sathishkumar, R. Balasubramanian, Interaction of rare earth elements with a brown marine alga in multi-component solutions, Desalination, 265 (2011) 54–59.
[11] S. Zakhama, H. Dhaouadi, F.M. Henni, Nonlinear modelisation of heavy metal removal from aqueous solution using *Ulva lactuca* algae, Bioresour. Technol., 102 (2011) 786–796.
[12] D. Bulgariu, L. Bulgariu, Equilibrium and kinetics studies of heavy metal ions biosorption on green algae waste biomass, Bioresour. Technol., 103 (2012) 489–493.
[13] M.M. Areco, S. Hanela, J. Duran, M.S. Afonso, Biosorption of Cu(II), Zn(II), Cd(II), and Pb(II) by dead biomasses of green alga *Ulva lactuta* and the development of a sustainable matrix for adsorption, J. Hazard. Mater., 213–214 (2012) 123–132.
[14] Y. Xiong, J. Xu, W. Shan, Z. Lou, D. Fang, S. Zang, G. Han, A new approach for rhenium(VII), recovery by using modified brown algae *Laminaria japonica* adsorbent, Bioresour. Technol., 127 (2013) 464–472.
[15] L. Deng, Y. Su, H. Su, X. Wang, X. Zhu, Sorption and desorption of lead (II) from waste water by green algae *Cladophora fascicularis*, J. Hazard. Mater., 143 (2007) 220–225.
[16] V.K. Gupta, A. Rastogi, Biosorption of lead from aqueous solution by green algae *Spirogyra* species: kinetics and equilibrium studies, J. Hazard. Mater., 152 (2008) 407–414.
[17] Buhani, Suharso, Immobilization of *Nannochloropsis* sp. biomass by sol-gel technique as adsorbent of metal ion Cu(II) from aqueous solution, Asian J. Chem., 21 (2009) 3799–3808.
[18] P.O. Harris, G.J. Ramelow, Binding of metal ions by particulate biomass derived from *Chlorella vulgaris* and *Scenedesmus quadricauda*, Environ. Sci. Technol., 24 (1990) 220–228.
[19] F. Veglio, F. Beolchini, L. Toro, Kinetic modeling of copper biosorption by immobilized biomass, Ind. Eng. Chem. Res., 37 (1998) 1107–1111.
[20] B. Volesky, Z.R. Holan, Biosorption of heavy metals, Biotechnol. Prog., 11 (1995) 235–250.
[21] Suharso, Buhani, Sumadi, Immobilization of *S. duplicatum* supported silica gel matrix and the application on adsorption–desorption of Cu(II), Cd(II) and Pb(II) ions, Desalination, 263 (2010) 64–69.
[22] Buhani, Suharso, Sumadi, Production of ionic imprinted polymer from *Nannochloropsis* sp biomass and its adsorption characteristics toward Cu(II) ion in solutions, Asian J. Chem., 24 (2012) 133–140.
[23] F. Lou, Y. Liu, X. Li, Z. Xuan, J. Ma, Biosorption of lead ion by chemically-modified biomass of marine brown algae *Laminaria japonica*, Chemosphere, 64 (2006) 1122–1127.
[24] W.O.W. Maznah, A.T. Al-Fawwaz, M. Surif, Biosorption of copper and zinc by immobilised and free algal biomass, and the effects of metal biosorption on the growth and cellular structure of *Chlorella* sp. and *Chlamydomonas* sp. isolated from rivers in Penang, Malaysia, J. Environ. Sci., 24 (2012) 1386–1393.
[25] E.F.C. Alcantara, E.A. Faria, D.V. Rodrigues, S.M. Evangelista, E. DeOliveira, L.F. Zara, D. Rabelo, A.G.S. Prado, Modification of silica gel by attachment of 2-mercaptobenzimidazole for use in removing Hg(II) from aqueous media: a thermodynamic approach, J. Colloid Interface Sci., 311 (2007) 1–7.
[26] N. Jiang, X. Chang, H. Zheng, Q. He, Z. Hu, Selective solid-phase extraction of nickel(II) using a surface-imprinted silica gel sorbent, Anal. Chim. Acta, 577 (2006) 225–231.
[27] C. Jeon, Adsorption characteristic of copper ions using magnetically modified medicinal stones, J. Ind. Eng. Chem., 17 (2011) 321–324.
[28] Q. Peng, Y. Liu, G. Zeng, W. Xu, C. Yang, J. Zhang, Biosorption of copper(II) by immobilizing *Saccharomyces cerevisiae* on the surface of chitosan-coated magnetic nanoparticle from aqueous solution, J. Hazard. Mater., 177 (2010) 676–682.
[29] H. Hu, Z. Wang, L. Pan, Synthesis of monodisperse Fe_3O_4@ silica core–shell microspheres and their application for removal of heavy metal ions from water, J. Alloys Compd., 492 (2010) 656–661.
[30] X. Xin, Q. Wei, J. Yang, L. Yan, R. Feng, G. Chen, B. Du, H. Li, Highly efficient removal of heavy metal ions by amine-functionalized mesoporous Fe_3O_4 nanoparticles, Chem. Eng. J., 184 (2012) 132–140.
[31] H. Bagheri, A. Afkhami, M. Saber-Tehrani, H. Khoshsafar, Preparation and characterization of magnetic nanocomposite of Schiff base/silica/magnetite as a preconcentration phase for the trace determination of heavy metal ions in water, food and biological samples using atomic absorption spectrometry, Talanta, 97 (2012) 87–95.
[32] Y. Lin, H. Chen, K. Lin, B. Chen, C. Chiou, Application of magnetic modified with amino groups to adsorb copper ion in aqueous solution, J. Environ. Sci., 23 (2011) 44–50.
[33] P.I. Girginova, A.L. Daniel-da-Silva, C.B. Lopes, P. Figueira, M. Otero, V.S. Amaral, E. Pereira, T. Trindade, Silica coated magnetite particles for magnetic removal of Hg^{2+} from water, J. Colloid Interface Sci., 345 (2010) 234–240.
[34] I. Mohmood, C.B. Lopes, I. Lopes, D.S. Tavares, A.M.V.M. Soares, A.C. Duarte, T. Trindade, I. Ahmad, E. Pereira, Remediation of mercury contaminated saltwater with functionalized silica coated magnetite nanoparticles, Sci. Total Environ., 557–558 (2016) 712–721.
[35] S. Bakhshayesh, H. Dehghan, Synthesis of magnetite-porphyrin nanocomposite and its application as a novel magnetic adsorbent for removing heavy cations, Mater. Res. Bull., 48 (2013) 2614–2624.

[36] Y.C. Chang, D.H. Chen, Preparation and adsorption properties of monodisperse chitosan-bound Fe_3O_4 magnetic nanoparticles for removal of Cu(II) ions, J. Colloid Interface Sci., 283 (2005) 446–451.
[37] A.Z.M. Badruddoza, Z.B.Z, Shawon, W.J.D. Tay, K. Hidayat, M.S. Uddin, Fe_3O_4/cyclodextrin polymer nanocomposites for selective heavy metals removal from industrial wastewater, Carbohydr. Polym., 91 (2013) 322–332.
[38] J. Zhang, S. Zhai, S. Li, Z. Xiao, Y. Song, Q. An, G. Tian, Pb(II) removal of Fe_3O_4@SiO_2–NH_2 core–shell nanomaterials prepared via a controllable sol–gel process, Chem. Eng. J., 215–216 (2013) 461–471.
[39] A.M. Donia, A.A. Atia, F.I. Abouzayed, Preparation and characterization of nano-magnetic cellulose with fast kinetic properties towards the adsorption of some metal ions, Chem. Eng. J., 191 (2012) 22–30.
[40] Y. Ren, M. Zhang, D. Zhao, Synthesis and properties Cu(II) ion imprinted composite adsorbent for selective removal of copper, Desalination, 228 (2008) 135–149.
[41] S.H. Araghi, M.H. Entezari, Amino-functionalized silica magnetite nanoparticles for the simultaneous removal of pollutants from aqueous solution, Appl. Surf. Sci., 333 (2015) 68–77.
[42] T.S. Anirudhan, F. Shainy, Adsorption behaviour of 2-mercaptobenzamide modified itaconic acid-grafted-magnetite nanocellulose composite for cadmium(II) from aqueous solutions, J. Ind. Eng. Chem., 32 (2015) 157–166.
[43] I. Sargin, G. Arslan, M. Kaya, Efficiency of chitosan-algal biomas composite microbeads at heavy metal removal, React. Funct. Polym., 98 (2016) 38–47.
[44] W. Jiang, X. Chen, Y. Niu, B. Pan, Spherical polystyrene-supported nano-Fe_3O_4 of high capacity and low-field separation for arsenate removal from water, J. Hazard. Mater., 243 (2012) 319–325.
[45] M.M. Montazer-Rahmati, P. Rabbani, A. Abdolali, A.R. Keshtkar, Kinetics and equilibrium studies on biosorption of cadmium, lead, and nickel ions from aqueous solutions by intact and chemically modified brown algae, J. Hazard. Mater., 185 (2011) 401–407.
[46] N. Chen, Z. Zhang, C. Feng, M. Zhu, D. Li, N. Sugiura, Studies on fluoride adsorption of iron-impregnated granular ceramics from aqueous solution, Mater. Chem. Phys., 125 (2011) 293–298.
[47] Z. Chen, W. Ma, M. Han, Biosorption of nickel and copper onto treated alga (*Undaria pinnatifida*): application of isotherm and kinetic models, J. Hazard. Mater., 155 (2008) 327–333.
[48] K. Srividya, K. Mohanty, Biosorption of hexavalent chromium from aqueous solution by *Catla catla* scales; equilibrium and kinetics studies, Chem. Eng. J., 155 (2009) 666–673.
[49] C. Gok, D. Turkozu, S. Aytas, Removal of Th(IV) from aqueous solution using bifungsional algae-yeast biosorbent, J. Radioanal. Nucl. Chem., 287 (2011) 533–541.
[50] M. Etienne, A. Walcarius, Analytical investigation of the chemical reactivity and stability of aminopropyl-grafted silica in aqueous medium, Talanta, 59 (2003) 1173–1188.
[51] V.K. Gupta, A. Rastogi, A. Nayak, Biosorption of nickel onto treated alga (*Oedogonium hatei*): application of isotherm and kinetic models, J. Colloid Interface Sci., 342 (2010) 533–539.
[52] H. Zhu, S. Jia, T. Wan, Y. Jia, H. Yang, J. Li, L. Yan, C. Zhong, Biosynthesis of spherical Fe_3O_4/bacterial cellulose nanocomposites as adsorbents for heavy metal ions, Carbohydr. Polym., 86 (2011) 1558–1564.
[53] Y.S. Ho, J.F. Porter, G. McKay, Equilibrium isotherm studies for the sorption of divalent metal ions onto peat: copper, nickel, and lead single component systems, Water Air Soil Pollut., 141 (2002) 1–33.
[54] J. Perić, M. Trgo, N. Vukojević Medvidović, Removal of zinc, copper and lead by natural zeolite—a comparison of adsorption isotherms, Water Res., 38 (2004) 1893–1899.
[55] I. Larraza, M. Lŏpez-Gŏnzales, T. Corrales, G. Marcelo, Hybrid materials: magnetite–polyethylenimine–montmorillonite, as magnetic adsorbents for Cr(VI) water treatment, J. Colloid Interface Sci., 385 (2012) 24–33.
[56] H. Niu, D. Zhang, S. Zhang, X. Zhang, Z. Meng, Y. Cai, Humic acid coated Fe_3O_4 magnetic nanoparticles as highly efficient Fenton-like catalyst for complete mineralization of sulfathiazole, J. Hazard. Mater., 190 (2011) 559–565.
[57] Y.G. Zhao, H.Y. Shen, S.D. Pan, M.Q. Hu, Synthesis, characterization and properties of ethylenediamine-functionalized Fe_3O_4 magnetic polymers for removal of Cr(VI) in wastewater, J. Hazard. Mater., 182 (2010) 295–302.
[58] A.E. Martell, R.D. Hancock, Metal Complexes in Aqueous Solution, Plenum Press, New York, 1996.
[59] A.Z.M. Badruddoza, A.S.H. Tay, P.Y. Tan, K. Hidayat, M.S. Uddin, Carboxymethyl-β-cyclodextrin conjugated magnetic nanoparticles as nano-adsorbents for removal of copper ions: synthesis and adsorption studies, J. Hazard. Mater., 185 (2011) 1177–1186.
[60] M.A. Karimi, M. Kafi, Removal, preconcentration and determination of Ni(II) from different environmental samples using modified magnetite nanoparticles prior to flame atomic absorption spectrometry, Arabian J. Chem., 8 (2015) 812–820.
[61] M.H.P. Wondracek, A.O. Jorgetto, A.C.P. Silva, J.R. Ivassechen, J.F. Schneider, M.J. Saeki, V.A. Pedrosa, W.K. Yoshito, F. Colauto, W.A. Ortiz, G.R. Castro, Synthesis of mesoporous silica-coated magnetic nanoparticles modified with 4-amino-3-hydrazino-5-mercapto-1,2,4-triazole and its application as Cu(II) adsorbent from aqueous samples, Appl. Surf. Sci., 367 (2016) 533–541.